

CHAPTER 5

Corrosion Kinetics and Applications of Electrochemistry to Corrosion

5.1 What Is Overpotential?

Thermodynamic principles can explain a corrosion situation in terms of the stability of chemical species and reactions associated with corrosion processes. However, thermodynamic principles cannot be used to predict corrosion currents or corrosion rates. In reality, polarization effects control the cathodic and anodic currents that are integral components of corrosion processes.

When two or more complementary processes such as those illustrated in Chap. 3 occur over a single metallic surface, the corrosion potential that results from such situations is a compromise between the various equilibrium potentials of all the anodic and cathodic reactions involved. The difference between the resultant potential (E) and each individual reaction equilibrium potential (E_{eq}) is called polarization and is quantified in terms of overpotential (η) described in Eq. (5.1):

$$\eta = E - E_{\text{eq}} \quad (5.1)$$

The polarization is said to be anodic when the anodic processes of the electrode are accelerated by moving the potential in the positive (noble) direction or cathodic when the cathodic processes are accelerated by moving the potential in the negative (active) direction. There are three distinct types of polarization and these are additive, as expressed in Eq. (5.2):

$$\eta_{\text{total}} = \eta_{\text{act}} + \eta_{\text{conc}} + iR \quad (5.2)$$

where η_{act} is the activation overpotential, a complex function describing the charge transfer kinetics of an electrochemical reaction.

η_{act} is always present and the main polarization component at small polarization currents or voltages.

η_{conc} is the concentration overpotential, a function describing the mass transport limitations associated with electrochemical processes. η_{conc} is dominant at larger polarization currents or voltages.

iR is the ohmic drop. This function takes into account the electrolytic resistivity of an environment when the anodic and cathodic elements of a corrosion reaction are separated by this environment while still electrically coupled.

Activation polarization is usually the controlling factor during corrosion in strong acids since both η_{conc} and iR are relatively small. Concentration polarization usually predominates when the concentration of the active species is low; for example, in dilute acids or in aerated waters where the active component, dissolved oxygen, is only present at very low levels. The ohmic drop will become an extremely important factor when studying corrosion phenomena for which there is a clear separation of the anodic and cathodic corrosion sites, for example, crevice corrosion. The ohmic drop is also an important variable in the application of protective methods such as anodic and cathodic protection that forces a potential shift of the protected structure by passing a current in the environment.

Knowing the kind of polarization which is occurring can be very helpful, since it allows an assessment of the determining characteristics of a corroding system. For example, if corrosion is controlled by concentration polarization, then any change that increases the diffusion rate of the active species (e.g., oxygen) will also increase the corrosion rate. In such a system, it would therefore be expected that agitating the liquid or stirring it would tend to increase the corrosion rate of the metal. However, if a corrosion reaction is activation controlled then stirring or increasing the agitation will have no effect on the corrosion rate.

5.2 Activation Polarization

Activation polarization is due to retarding factors that are an inherent part of the kinetics of all electrochemical reactions. For example, consider the evolution of hydrogen gas illustrated previously in Chap. 3 and described by Eq. (5.3):



While this reaction seems to be relatively simple, the rate at which hydrogen ions are transformed into hydrogen gas is in reality a

function of several factors, including the rate of electron transfer from a metal to hydrogen ions. In fact, there is a wide variability in this transfer rate of electrons on various metals and, as a result, the rate of hydrogen evolution from different metal surfaces can vary greatly.

The exchange current density (i_0) is surely the single most important variable that explains the large differences in the rate of hydrogen production on metallic surfaces. Table 5.1 contains the approximate exchange current density for the reduction of hydrogen ions on a range of materials. Note that the value for the exchange current density of hydrogen evolution on platinum is approximately 10^{-2} A/cm² whereas on mercury and lead it is 10^{-13} A/cm², eleven orders of magnitude difference for the rate of this particular reaction, or one hundred billion times easier on platinum than on mercury or lead!

This is the reason why mercury is often added to power cells such as the popular alkaline primary cells to stifle the thermodynamically favored production of gaseous hydrogen and prevent unpleasant incidents. This is also why lead acid batteries (car batteries) can provide power in a highly acidic environment in a relatively safe manner unless excessive charging currents are used.

Even so, the exchange current density remains an elusive parameter that may change rapidly with changing conditions at a metallic surface being naturally modified during its exposure in a given environment. One problem is that there is no simple method to estimate the exchange current density for a specific system. The exchange current density must be determined experimentally by scanning the potential with a laboratory setup such as shown in Fig. 5.1. In this experimental arrangement a potentiostat/galvanostat power controller is used to pass current through the sample, or working electrode (W), and an auxiliary electrode (AUX) immersed in solution while monitoring the potential of the working electrode with a reference electrode and a Luggin capillary.

Metal	$\log_{10} i_0$ (A/cm ²)
Pb, Hg	-13
Zn	-11
Sn, Al, Be	-10
Ni, Ag, Cu, Cd	-7
Fe, Au, Mo	-6
W, Co, Ta	-5
Pd, Rh	-4
Pt	-2

TABLE 5.1 Approximate Exchange Current Density (i_0) for the Hydrogen Oxidation Reaction on Different Metals at 25°C

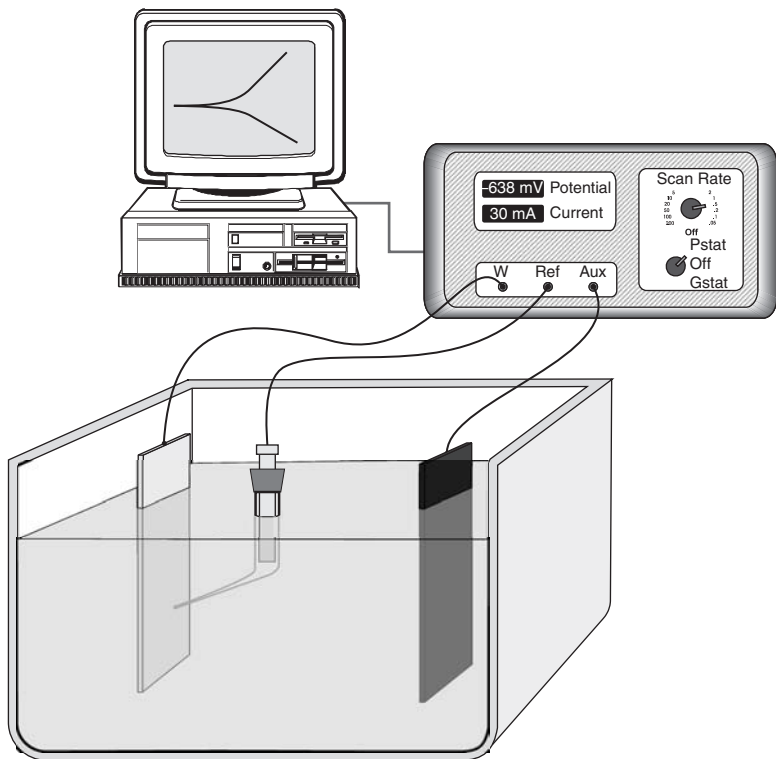


FIGURE 5.1 Electrochemical instrumentation to carry out potentiodynamic measurements in which a potentiostat/galvanostat power controller is used to pass current through the sample or working electrode (W) and an auxiliary electrode (AUX), while monitoring the potential of the working electrode with a reference electrode.

The following theory explains the basic mathematics that may be used to extract the exchange current density from the results obtained. A general representation of the polarization of an electrode supporting one specific reaction is given in the Butler-Volmer equation (5.4):

$$i_{\text{reaction}} = i_0 \left\{ \exp\left(-\beta \frac{nF}{RT} \eta_{\text{reaction}}\right) - \exp\left((1-\beta) \frac{nF}{RT} \eta_{\text{reaction}}\right) \right\} \quad (5.4)$$

where i_{reaction} is the anodic or cathodic current
 β is the charge transfer barrier (symmetry coefficient) for the anodic or cathodic reaction, usually close to 0.5
 n is the number of participating electrons
 R is the gas constant, that is, $8.314 \text{ J mol}^{-1} \text{ K}^{-1}$
 T is absolute temperature (K)
 F is $96,485 \text{ C}/(\text{mol of electrons})$

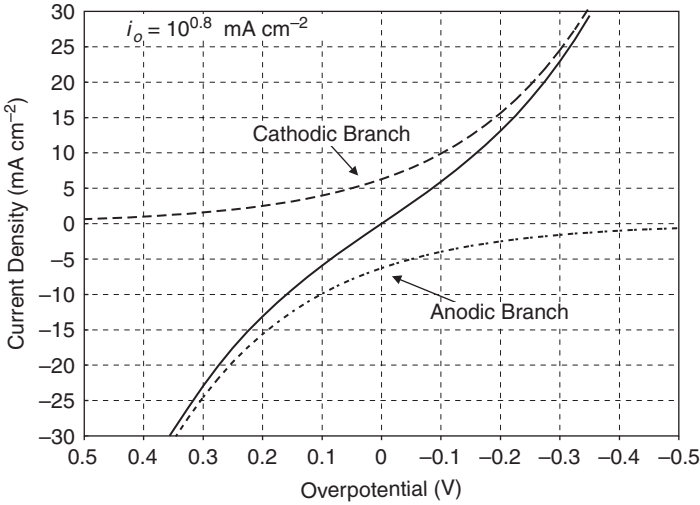


FIGURE 5.2 Current versus overpotential polarization plot of the ferric/ferrous ion reaction on palladium showing both the anodic and cathodic branches of the resultant current behavior.

The presence of two polarization branches in a single reaction expressed in Eq. (5.4) is illustrated in Fig. 5.2 for the polarization of a palladium electrode immersed in a solution containing similar concentrations of ferric (Fe^{3+}) and ferrous (Fe^{2+}) ions with a completely reversible reaction described in Eq. (5.5):



When η_{reaction} is cathodic, that is, negative, the second term in the Butler-Volmer equation becomes negligible and the cathodic current density (i_c) can be expressed by a simpler equation [Eq. (5.6)] and its logarithm [Eq. (5.7)]:

$$i_{\text{reaction}} = i_c = i_0 \exp\left(-\beta \frac{nF}{RT} \eta_{\text{reaction}}\right) \quad (5.6)$$

$$\eta_{\text{reaction}} = \eta_c = b_c \log_{10}\left(\frac{i_c}{i_0}\right) \quad (5.7)$$

where b_c is the cathodic Tafel coefficient described in Eq. (5.8) that can be obtained from the slope of a plot of η against $\log |i|$, with the intercept yielding a value for i_0 as shown in Fig. 5.3.

$$b_c = -2.303 \frac{RT}{\beta nF} \quad (5.8)$$

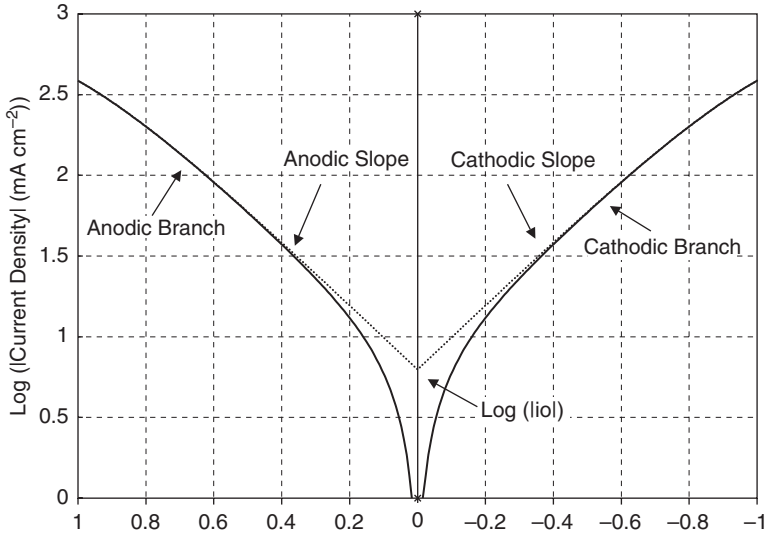


FIGURE 5.3 Plot of η against $\log |i|$ or Tafel plot showing the exchange current density can be obtained with the intercept.

Similarly, when η_{reaction} is anodic, that is, positive, the first term in the Butler-Volmer equation becomes negligible and the anodic current density (i_a) can be expressed by Eq. (5.9) and its logarithm in Eq. (5.10), with b_a obtained by plotting η_{reaction} versus $\log |i|$ [Eq. (5.11)]:

$$i_{\text{reaction}} = i_a = -i_0 \exp\left((1-\beta) \frac{nF}{RT} \eta_{\text{reaction}}\right) \quad (5.9)$$

$$\eta_a = b_a \log_{10} \left(\frac{|i_a|}{i_0}\right) \quad (5.10)$$

$$b_a = 2.303 \times \frac{RT}{\beta nF} \quad (5.11)$$

5.3 Concentration Polarization

Concentration polarization is the polarization component caused by concentration changes in the environment adjacent to the surface as illustrated in Fig. 5.4. When a chemical species participating in a corrosion process is in short supply, the mass transport of that species to the corroding surface can become rate controlling. A frequent case of concentration polarization occurs when the cathodic processes depend on the reduction of dissolved oxygen since it is usually in low concentration, that is, in parts per million (ppm) as shown in Table 5.2 [1].

Temperature (°C)	Volume (cm ³)*	Concentration (ppm)	Concentration (M) (μmol L ⁻¹)
0	10.2	14.58	455.5
5	8.9	12.72	397.4
10	7.9	11.29	352.8
15	7.0	10.00	312.6
20	6.4	9.15	285.8
25	5.8	8.29	259.0
30	5.3	7.57	236.7

* cm³ at 0°C per kg of water.

TABLE 5.2 Solubility of Oxygen in Air-Saturated Water

As illustrated in Fig. 5.5, mass transport to a surface is governed by three forces, that is, diffusion, migration, and convection. In the absence of an electrical field the migration term is negligible since it only affects charged ionic species while the convection force disappears in stagnant conditions. For purely diffusion controlled

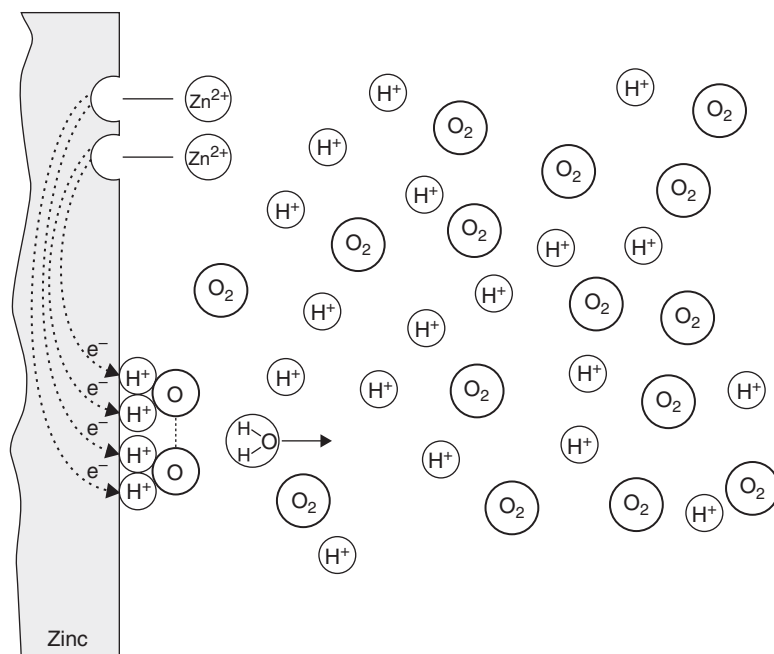


FIGURE 5.4 Concentration changes in the vicinity of an electrode causing a concentration polarization effect.

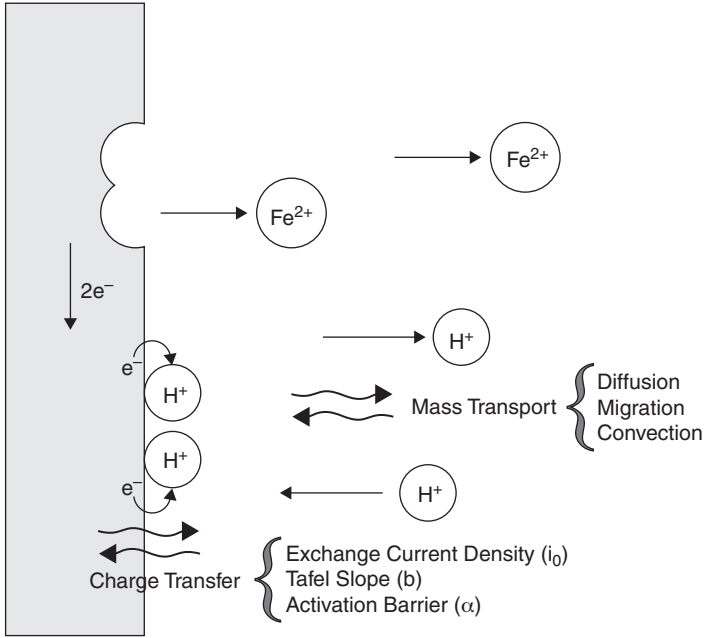


FIGURE 5.5 Graphical representation of the processes occurring at an electrochemical interface.

mass transport, the flux of a species O to a surface from the bulk is described with Fick's first law in Eq. (5.12):

$$J_O = -D_O \left(\frac{\delta C_O}{\delta x} \right) \tag{5.12}$$

where J_O is the flux of species O ($\text{mol s}^{-1} \text{cm}^{-2}$)

D_O is the diffusion coefficient of species O ($\text{cm}^2 \text{s}^{-1}$)

δC_O is the concentration gradient of species O across the interface between the metallic surface and the bulk environment (mol cm^{-3})

δx is the Nernst diffusion layer or diffuse layer (cm)

Table 5.3 contains values for D_O of some common ions. For more practical situations the diffusion coefficient can be approximated with the help of Eq. (5.13), that relates D_O to the viscosity of the solution (μ) and absolute temperature:

$$D_O = \frac{T \cdot A}{\mu} \tag{5.13}$$

where A is a constant for the system.

Cation	$D \times 10^5$ ($\text{cm}^2 \text{s}^{-1}$)	Anion	$D \times 10^5$ ($\text{cm}^2 \text{s}^{-1}$)
H^+	9.30	OH^-	5.25
Li^+	1.03	F^-	1.47
Na^+	1.33	Cl^-	2.03
K^+	1.95	NO_3^-	1.90
Ca^{2+}	0.79	ClO_4^-	1.79
Cu^{2+}	0.71	SO_4^{2-}	1.06
Zn^{2+}	0.70	CO_3^{2-}	0.92
O_2	2.26	HSO_4^-	1.33
H_2O	2.44	HCO_3^-	1.11

TABLE 5.3 Diffusion Coefficients of Selected Ions at Infinite Dilution in Water at 25°C

Figure 5.6 illustrates the concentration-distance profile at the electrode surface approximated by a simple gradient. In this diagram the metallic surface is positioned at the ordinate axis while the x-axis expresses the distance away from the electrode and the y-axis the concentration of the chemical species being reacted. For well-mixed solutions, the concentration is constant in the bulk or convective region.

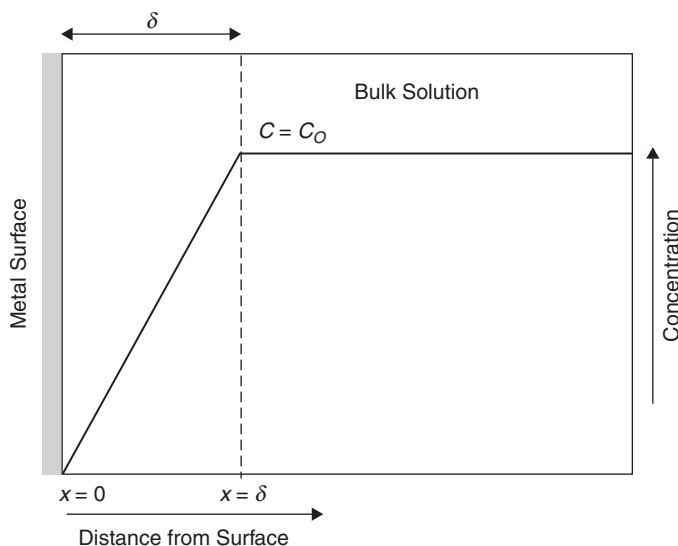


FIGURE 5.6 Nernst diffusion layer for a limiting current situation.

This is represented by the horizontal line where $C = C_O$. There is also a region where the concentration drops, falling to zero at the electrode surface. The Nernst diffusion layer associated with this drop has a specific thickness (δ) that depends upon the nature of the solution into which it extends. For stirred aqueous solutions the thickness of the diffusion layer varies between 0.01 and 0.001 mm.

For a chemical species O that is consumed by the cathodic reaction at the corroding surface, the concentration gradient ($\delta C_O / \delta x$) is greatest when the concentration of that species is completely depleted at the surface, that is, $C_O = 0$. It follows that the cathodic current is limited in that condition, as expressed by Eq. (5.14).

$$i_c = i_L = -nFD_O \frac{C_O^{\text{bulk}}}{\delta} \quad (5.14)$$

For intermediate cases, that is, when the cathodic current is smaller than i_L , η_{conc} can be evaluated using an expression [Eq. (5.15)] derived from Nernst equation:

$$\eta_{\text{conc}} = \frac{2.303 \times RT}{nF} \log_{10} \left(1 - \frac{i}{i_L} \right) \quad (5.15)$$

where $2.303 \times R \times T / F = 0.059 \text{ V}$ when $T = 298.16 \text{ K}$.

5.4 Ohmic Drop

The ohmic overpotential appears in Eq. (5.2) as the simple product of a resistance and a current between the anodic and cathodic sites of a corrosion process. For many corrosion situations these sites are adjacent to each other and the ohmic drop is negligible, particularly so when the environment itself is a good electrolytic conductor, that is, seawater. However, there are special conditions where the separation of the anodic and cathodic sites can be an important factor in the corrosion progress, for example, galvanic corrosion, or even an integral part of a particular protection scheme, for example, anodic and cathodic protection.

5.4.1 Water Resistivity Measurements

The conductivity of an environment can itself be a complex function. When a salt dissociates, the resulting ions interact with surrounding water molecules to form charged clusters known as solvated ions. These ions can move through the solution under the influence of an externally applied electric field. Such motion of charge is known as ionic conduction and the resulting conductance is the reciprocal function of the resistance of an environment.

The dependence upon the size and shape of the conductor can be corrected by using the resistivity ρ rather than the resistance R , as

Water	ρ ($\Omega \text{ cm}$)
Pure water	20,000,000
Distilled water	500,000
Rain water	20,000
Tap water	1000–5000
River water (brackish)	200
Sea-water (coastal)	30
Sea-water (open sea)	20–25

TABLE 5.4 Resistivity of Some Typical Waters

expressed in Eq. (5.16) for the simple cell shown in Fig. 5.7. Table 5.4 lists some typical values of water resistivity [1].

$$\rho = \frac{R}{\left(\frac{\ell}{A}\right)} \quad (5.16)$$

where R is the measured resistance across the cell

A is the cross-sectional area of each electrode, provided that

both electrodes have the same dimensions

ℓ is the gap separating the electrodes in Fig. 5.7

The ratio (ℓ/A) is also called the cell constant or *shape factor* and has units of cm^{-1} or m^{-1} . A variant of the electrochemical cell shown in Fig. 5.7 is commonly used to evaluate the conductivity of a solution between two electrodes by using an alternating current technique.

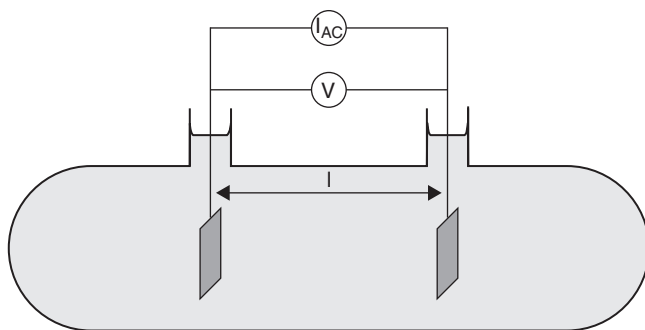


FIGURE 5.7 Schematic of a conductivity cell containing an electrolyte and two inert electrodes of surface A parallel to each other and separated by distance ℓ .

Other geometries would require the calculation of appropriate cell constants. The cell constant of an electrochemical cell with two concentric tubes as electrodes would be, for example, expressed by Eq. (5.17). Such an arrangement is a common design in the production of domestic water heaters in which a central sacrificial magnesium anode is inserted typically in the center of the hot-water tank to protect the surrounding tank material.

$$\text{Cell constant} = \frac{1}{2\pi h} \ln\left(\frac{r_2}{r_1}\right) \quad (5.17)$$

where h is the height of the cylindrical tank

r_2 is the internal tank radius

r_1 is the radius of the sacrificial anode

The ohmic drop can be minimized, when carrying out electrochemical tests, by placing the reference electrode in a Luggin capillary brought as close as possible to the surface being monitored (Fig. 5.8). Additionally, the Luggin capillary allows sensing of the solution potential close to the working electrode without the adverse shielding effects that may be caused when the reference electrode is positioned in front of the surface being monitored. A Luggin capillary

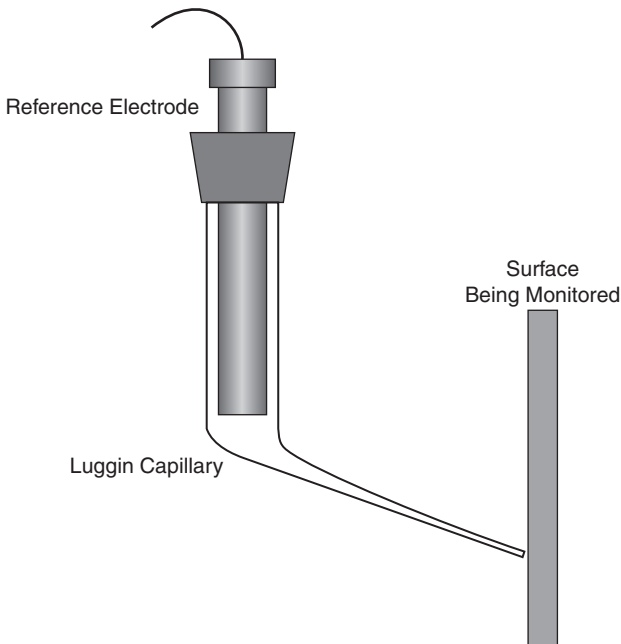


FIGURE 5.8 Schematic of a Luggin capillary to position a reference electrode in close proximity to an electrochemical cell's working electrode.

can be made of any material provided it is inert to the electrolytic environment. It basically consists of a bent tube generally filled with the test solution with a large enough opening to accommodate a reference electrode at one end and a usually much smaller opening at the other end to provide diffusional movement of the electrolyte.

5.4.2 Soil Resistivity Measurements

Soil resistivity is a function of soil moisture and the concentrations of ionic soluble salts and is considered to be the most comprehensive indicator of a soil's corrosivity. Typically, the lower the resistivity, the higher will be the corrosivity as discussed in more details in Chap. 10. Typically, soil resistivity decreases with increasing water content and the concentration of ionic species. Sandy soils, for example, are high up on the resistivity scale and therefore considered the least corrosive while clay soils are excellent at retaining water and at the opposite end of the corrosivity spectrum.

Four-Pin Method (Wenner Method)

Field soil resistivity measurements are most often conducted using the Wenner four-pin method and a soil resistance meter following the principles laid out by Wenner nearly one century ago [2]. The Wenner method requires the use of four metal probes or electrodes, driven into the ground along a straight line, equidistant from each other, as shown in Fig. 5.9 and Fig. 5.10. Soil resistivity is a relatively simple function derived from the voltage drop between the center pair of pins (P1 and P2 in Fig 5.9), with current flowing between the two outside pins (C1 and C2 in Fig 5.9) assuming that the measured resistivity is a measure of the hemispherical volume of earth probed by the central pins.

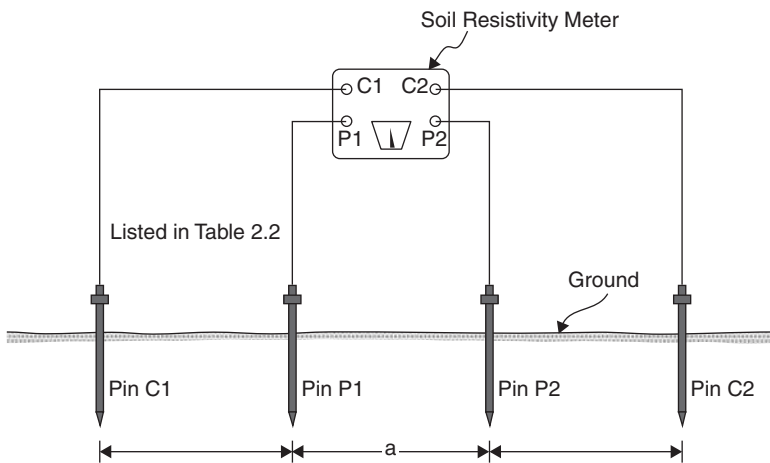


FIGURE 5.9 Wenner four-pin soil resistivity test setup.



(a)



(b)

FIGURE 5.10 Four-pin soil resistivity measurements being made; (a) field setup and (b) close-up on the instrument. (Courtesy of Tinker & Rasor)

An alternating current from the soil resistance meter causes current to flow through the soil, between pins C1 and C2 and the voltage or potential is measured between pins P1 and P2. Resistivity of the soil is then computed from the instrument reading, according to the following formula [1]:

$$\rho = 2\pi aR \quad (5.18)$$

where ρ is the soil resistivity (Ω cm)
 a is the distance between probes (cm)
 R is the soil resistance (Ω), instrument reading
 π is 3.1416

The resistivity values obtained represent the average resistivity of the soil to a depth equal to the pin spacing. Resistance measurements are typically performed to a depth equal to that of the buried system (pipeline) being evaluated. Typical probe spacing is in increments of 0.5 to 1 m.

If the line of soil pins used when making four-pin resistivity measurements is closely parallel to a bare underground pipeline or other metallic structure, the presence of the bare metal may cause the indicated soil resistivity values to be lower than it actually is. Because a portion of the test current will flow along the metallic structure rather than through the soil, measurements along a line closely parallel to pipelines should therefore be avoided.

The recorded values from four-pin resistivity measurements can be misleading unless it is remembered that the soil resistivity encountered with each additional depth increment is averaged, in the test, with that of all the soil in the layers above. With experience, much can be learned about the soil structure by inspecting series of readings to increasing depths. The indicated resistivity to a depth equal to any given pipe spacing is a weighted average of the soils from the surface to that depth. Trends can be illustrated best by inspecting the sets of soil resistivity readings in Table 5.5.

Pin Spacing (m)	Pin Pacing (F)	Soil Resistivity (Ω cm)			
		Set A	Set B	Set C	Set D
0.76	2.5	960	1100	3300	760
1.5	5	965	1000	2200	810
2.3	7.5	950	1250	1150	1900
3.0	10	955	1500	980	3800
3.8	12.5	960	1610	840	6900
4.6	15	955	1710	780	12,500

TABLE 5.5 Examples of Soil Resistivity Readings Using Four-Pin Method

The first set of data in Table 5.5, Set A, represents uniform soil conditions. The average of the readings shown ($\sim 960 \Omega \text{ cm}$) represents the effective resistivity that may be used for design purposes for impressed current groundbeds or galvanic anodes.

Data Set B represents low-resistivity soils in the first few feet. There may be a layer of somewhat less than $1000 \Omega \text{ cm}$ around the 1.5 m depth level. Below 1.5 m, however, higher-resistivity soils are encountered. Because of the averaging effect the actual resistivity at 2.3 m deep would be higher than the indicated $1250 \Omega \text{ cm}$ and might be in the order of $2500 \Omega \text{ cm}$ or more. Even if anodes were placed in the lower-resistivity soils, there would be resistance to the flow of current downward into the mass of the earth.

If designs are based on the resistivity of the soil in which the anodes are placed, the resistance of the completed installation will be higher than expected. The anodes will perform best if placed in the lower resistance soil. However, the effective resistivity used for design purposes should reflect the higher resistivity of the underlying areas. In this instance, where increase is gradual, using horizontal anodes in the low-resistivity area and a figure of effective resistivity of $\sim 2500 \Omega \text{ cm}$ should result in a conservative design.

Data Set C represents an excellent location for anode location even though the surface soils have relatively high resistivity. It would appear from this set of data that anodes located $>1.5 \text{ m}$ deep, would be in low-resistivity soil of $\sim 800 \Omega \text{ cm}$, such a figure being conservative for design purposes. A lowering resistivity trend with depth, as illustrated by this set of data, can be relied upon to give excellent groundbed performance.

Data Set D is the least favorable of these sample sets of data. Low-resistivity soil is present at the surface but the upward trend of resistivity with depth is immediate and rapid. At the 2.3 m depth, for example, the resistivity could be tens of thousands of ohm-centimeters. One such situation could occur where a shallow swampy area overlies solid rock. Current discharged from anodes installed at such a location will be forced to flow for relatively long distances close to the surface before electrically remote earth is reached. As a result, potential gradients forming the area of influence around an impressed current groundbed can extend much farther than those surrounding a similarly sized groundbed operating at the same voltage in more favorable locations such as those represented by data Sets A and C.

Alternate Soil Resistivity Methods

In the two-pin (Shepard's Canes) method of soil resistivity measurement, the potential drop is measured between the same pair of electrodes used to supply the current [3]. As shown in Fig. 5.11, the probes are placed 0.3 m apart. If the soil is too hard for the probes to penetrate, the reading is taken at the bottom of two augured holes.

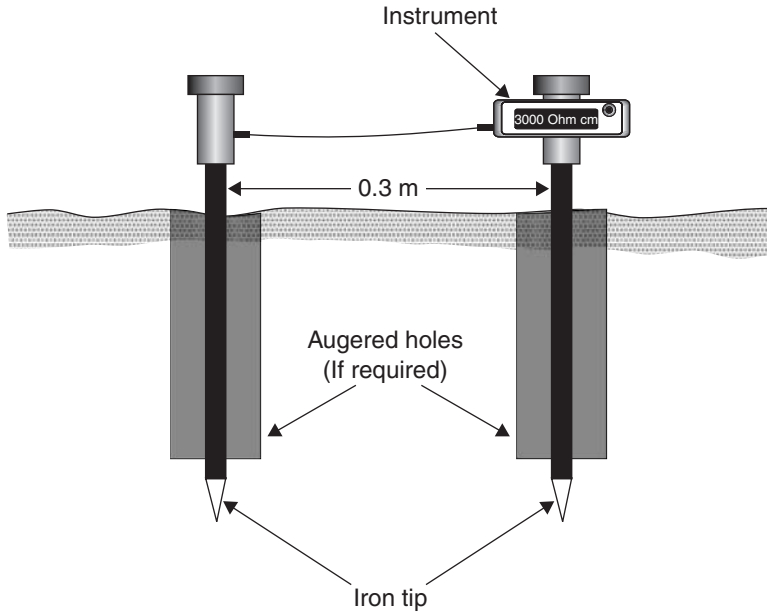


FIGURE 5.11 Two-pin (Shepard's Canes) method for soil resistivity measurements.

The instrument is calibrated for a probe spacing of 0.3 m and gives a reading directly in ohm cm. Although this method is less accurate than the four-pin method and measures the resistivity of the soil only near the surface, it is often used for preliminary surveys, as it is quicker than the four-pin method.

A soil rod is essentially a two-pin resistivity-measuring device where the electrodes are both mounted on a single rod, as shown in Fig. 5.12. As in the other two-pin method, the resistivity of the soil to a very shallow depth is measured. Also, the soil must be soft enough to allow penetration of the rod. Measurements using the soil rod, however, can be taken quickly when measuring in soft soil.

When it is impractical to make field measurements of soil resistivity, soil samples can be taken and the resistivity of the sample can be determined by using a soil box. As shown in Fig. 5.13, the method of measurement is essentially the four-pin method. Metal contacts in each end of the box pass current through the sample.

Potential drop is measured across probes inserted into the soil. The resistivity is calculated using constants provided with the particular geometry of soil box being used. Due to the disturbance of the soil during sampling and possible drying out of the soil during shipment, this method of soil resistivity measurement is less likely to represent true, in-place soil resistivity than an actual field test.

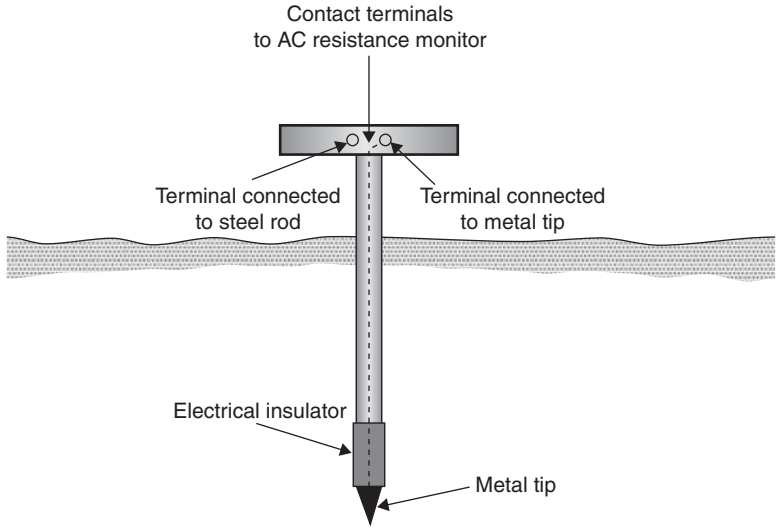


FIGURE 5.12 Soil rod method for soil resistivity measurements.



FIGURE 5.13 Soil box and resistivity equipment. (Courtesy of Tinker & Rasor)

5.5 Graphical Presentation of Kinetic Data (Evans Diagrams)

The use of polarization curves for the study of corrosion reactions can be traced back to the 1930s with the work of Wagner and Traud [4]. However the representation of the mixed potential behavior is often associated with Professor Evans who has popularized this representation of corrosion polarization measurements [5].

These polarization diagrams can be quite useful for describing or explaining parallel corrosion processes. According to the mixed-potential theory underlying these diagrams, any electrochemical reaction can be algebraically divided into separate oxidation and reduction reactions with no net accumulation of electrical charge. Under these circumstances the net measurable current is zero and the corroding metal is charge neutral, that is, all electrons produced by the corrosion of a metal have to be consumed by one or more cathodic processes.

In order to model a corrosion situation with mixed potential diagrams, one must first gather the information concerning the (1) activation overpotential for each corrosion process involved and (2) any additional information for processes that could be affected by concentration overpotential. The following sections present some examples that illustrate how the mixed potential theory may be used to explain simple cases where corrosion processes are purely activation controlled or cases where concentration controls at least one of the corrosion processes.

5.5.1 Activation Controlled Processes

For purely activation controlled processes, each reaction can be described by a straight line on an E versus $\text{Log } i$ plot, with positive Tafel slopes for anodic processes and negative Tafel slopes for cathodic processes.

The following example illustrates the polarization behavior of carbon steel in a deaerated solution maintained at 25°C with a pH of zero. The solid line in Fig. 5.14 is the polarization plot itself and the dotted lines in this figure represent the anodic reaction in Eq. (5.19) and the cathodic reaction in Eq. (5.20) that describe the corrosion behavior of steel in these conditions. These lines are extrapolated from the linear sections of the plot on either the anodic or cathodic sides of the curve.



While it is relatively easy to estimate the corrosion potential (E_{corr}) from the sharp peak observed at -0.221 V vs. standard

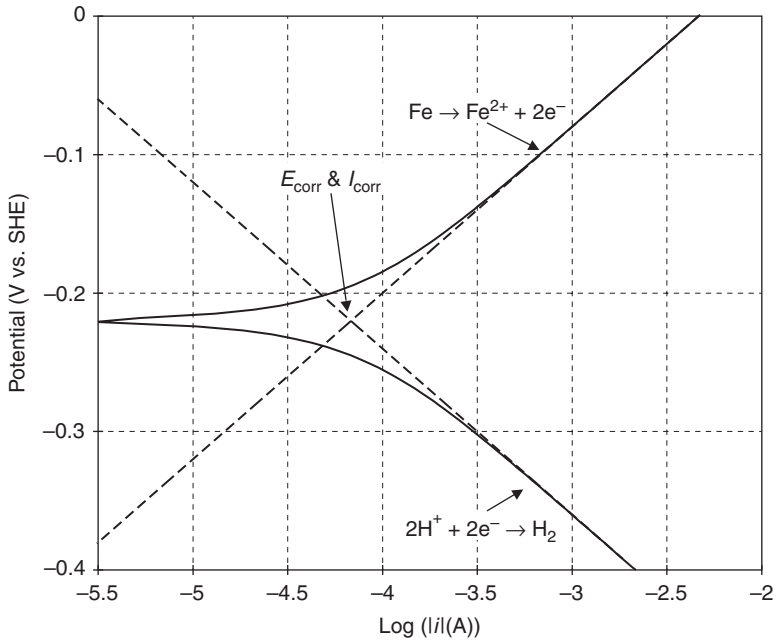


FIGURE 5.14 Polarization behavior of carbon steel in a deaerated solution maintained at 25°C and a pH of zero.

hydrogen electrode (SHE), when the current crosses zero (infinity on a log scale), the projected dotted lines are required to find the intercept indicating where the cathodic and anodic currents actually cancel each other. The corrosion current density (i_{corr}) can be obtained by dividing the anodic current by the surface area of the specimen, 1 cm² in the present case. According to the conversion table presented earlier in Chap. 3 (Table 3.2), the current density of 67 μA cm⁻² evaluated in this example corresponds to a penetration rate of 0.8 mm y⁻¹.

The second example shows the carbon steel polarization behavior when exposed to a deaerated solution maintained at 25°C and pH of five. The mixed potential diagram of this system is shown in Fig. 5.15. The shift of the E_{corr} to a more negative value of -0.368 V vs SHE should be noted. The modeled projected lines provide an estimate of the corrosion current density of 4 μA cm⁻² in this case and this current translates into a penetration rate of 0.05 mm y⁻¹.

5.5.2 Concentration Controlled Processes

When one of the reactions is limited by the rate of transport of the reactant to the metallic surface being corroded, the situation increases in complexity as illustrated in the polarization plot of the system in Fig. 5.16. The system represented here is similar to the previous one,

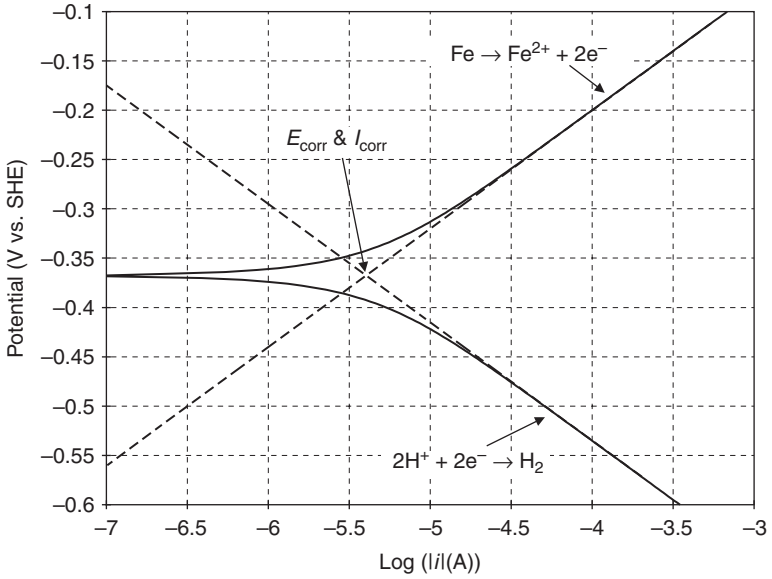


FIGURE 5.15 Polarization behavior of carbon steel in a deaerated solution maintained at 25°C and a pH of five.

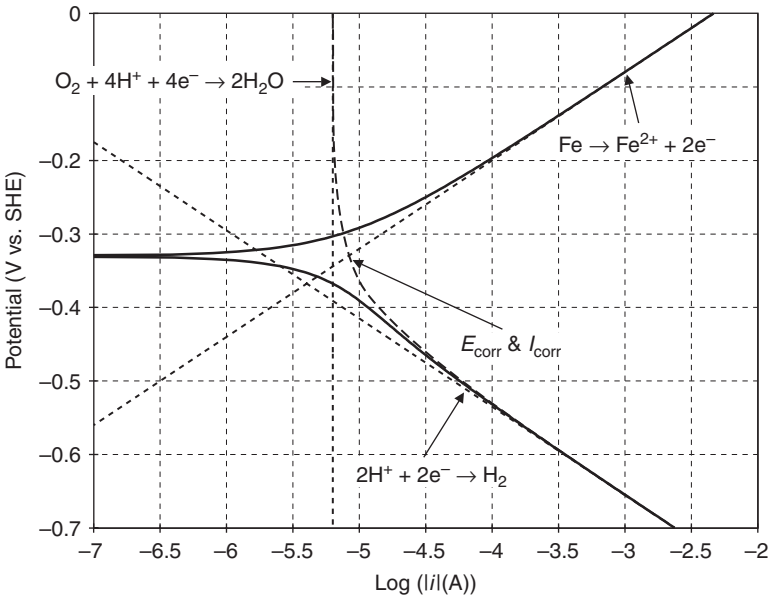


FIGURE 5.16 Polarization behavior of carbon steel in a stagnant aerated solution maintained at 25°C and a pH of five.

that is, pH of five at 25°C, with the exception that the environment is aerated and stagnant. In this situation the reduction of oxygen shown in Eq. (5.21) now becomes a possible second cathodic reaction.



In order to model the polarization plot, the total cathodic current corresponding to the sum of the currents of the hydrogen reaction and oxygen reduction has to be balanced by the single anodic current. The intercept where the opposing currents are balanced occurs at an E_{corr} of -0.33 V vs. SHE and, since the surface area is still 1 cm^2 , an i_{corr} of $8.2 \mu\text{A cm}^{-2}$ or 0.1 mm y^{-1} . It should be noted that the current for the reduction of oxygen is constant across the potential range shown in Fig. 5.16 and has the value of $6.3 \mu\text{A cm}^{-2}$.

The reduction of oxygen depends, among other factors, on the level of agitation of the environment. If the limiting current of this reaction is now increased through agitation by a tenfold factor to reach the value of $63 \mu\text{A cm}^{-2}$ a new situation emerges as depicted in Fig. 5.17. The marked positive shift of E_{corr} , now -0.224 V vs. SHE, is accompanied by a marked increase in current density, now of $63 \mu\text{A cm}^{-2}$ or 0.8 mm y^{-1} .

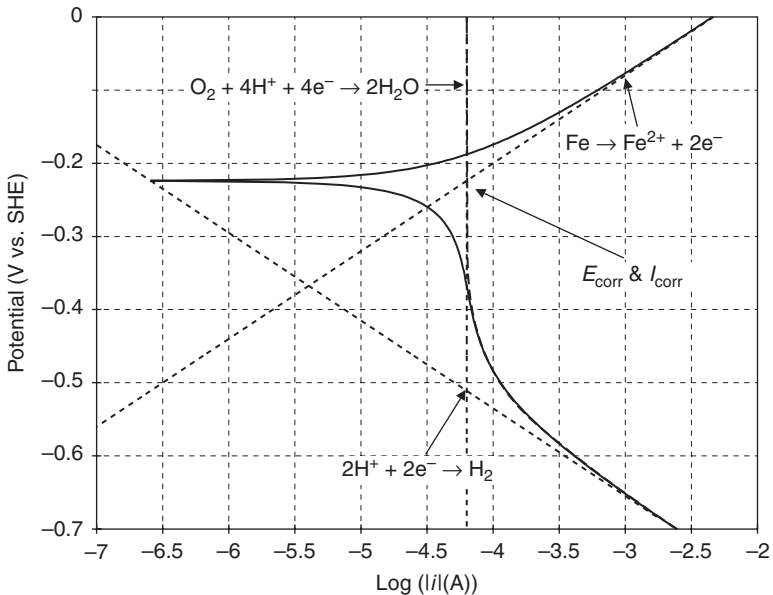


FIGURE 5.17 Polarization behavior of carbon steel in an agitated aerated solution maintained at 25°C and a pH of five.